Measurement 111 (2017) 197–207

Contents lists available at ScienceDirect

Measurement

journal homepage: www.elsevier.com/locate/measurement

Quantification of concrete railway sleeper bending moments using surface strain gauges

J. Riley Edwards [a,*], Zhengboyang Gao [a], Henry E. Wolf [b], Marcus S. Dersch [a], Yu Qian [a]

[a] Rail Transportation and Engineering Center – RailTEC, Department of Civil and Environmental Engineering, University of Illinois at Urbana-Champaign, 1243 Newmark Civil Engineering Laboratory, MC-250, 205 N. Mathews Ave., Urbana, IL 61801, United States
[b] FIGG Bridge Group, Western Regional Office, 9635 Maroon Circle, Suite 125, Englewood, CO 80112, United States

ARTICLE INFO

Article history:
Received 1 May 2017
Received in revised form 23 June 2017
Accepted 13 July 2017
Available online 20 July 2017

Keywords:
Concrete sleeper
Field instrumentation
Rail engineering
Flexural strength
Bending moments
Strain gauges

ABSTRACT

As the use of concrete sleepers increases for heavy-haul freight railroad and rail transit applications in North America, it is becoming more critical to quantify their flexural performance under revenue service traffic in an effort to improve sleeper design and maintenance practices. The objective of improving sleeper design and performance is achieving longer service lives, lower life cycle costs, and fewer in-service failures. Presently, center cracking is one of the most common factors limiting the service life of concrete sleepers in North America, and rail seat cracking has also been documented as a performance concern. Improving the understanding of sleeper flexure can help reduce the occurrences of cracked sleepers by ensuring designs are adequate for the field conditions that are encountered. Additionally, previous laboratory research conducted at the University of Illinois at Urbana-Champaign (UIUC) found that sleeper flexure magnitude is highly dependent on support conditions. To date, few methods have been proposed to accurately quantify the in-service field bending moments of concrete sleepers and their variability due to support conditions and other factors. A method using concrete surface strain gauges has been developed, deployed, and validated by UIUC for quantification of sleeper bending moments. This method has been successfully deployed in the laboratory and in seven field locations, providing flexural demand data that can be used for the design of concrete sleepers. This paper will present the aforementioned instrumentation methodology and results from one field installation in which surface strain gauges were installed on ten concrete sleepers on a high-tonnage, heavy-haul freight railroad with the objective of quantifying sleeper-to-sleeper bending moment variability.

1. Introduction

Throughout the world, the majority of railroad track infrastructure is supported by ballast. A ballasted track system typically consists of the rail, fastening systems, sleepers, ballast, sub-ballast, and subgrade [1]. Currently in North America, concrete is the second most common material used in the manufacture of sleepers, but concrete is the dominant sleeper material used internationally [2–4]. Additionally, pre-tensioning is the most common practice used for the manufacture of concrete sleepers in North America, with some post-tensioning operations beginning to emerge [5]. Due to the increased flexural strength, ductility, and resistance to cracking produced by the "pre-tensioned" steel wires [6], prestressed concrete sleepers can withstand the high dynamic loading environment imparted by passing trains. Additionally, in the United States, prestressed concrete sleepers are commonly used in the most demanding service conditions with high curvature, steep grades, heavy freight tonnage, and high and higher-speed passenger train traffic [4,5,7].

According to an international survey of railroads, concrete sleeper manufacturers, and researchers, sleeper cracking from center binding support under the center of member, and not the ends) was ranked as one of the most critical problems with concrete sleepers that can limit their service life [5]. Additionally, rail seat cracks have also been cited as a performance-related challenge for concrete sleepers and have been the subject of considerable research [8,9]. Because of the increasing application of prestressed concrete sleepers in demanding operating environments, it is important to understand the factors that cause the sleepers to crack at the rail seat and center. The input loading, support configurations, and resulting bending experienced by the sleeper can be quantified through laboratory experimentation, finite element (FE)

* Corresponding author.
E-mail addresses: jedward2@illinois.edu (J.R. Edwards), zgao9@illinois.edu (Z. Gao), hwolf@figgbridge.com (H.E. Wolf), mdersch2@illinois.edu (M.S. Dersch), yuqian1@illinois.edu (Y. Qian).

http://dx.doi.org/10.1016/j.measurement.2017.07.029
0263-2241/

modeling, and field experimentation, and a broad concrete sleeper research effort funded by the Federal Railroad Administration (FRA) conducted by the Rail Transportation and Engineering Center (RailTEC) at the University of Illinois at Urbana-Champaign (UIUC) aimed to quantify these [10–12].

While useful input data related to the mechanistic design [13] of sleepers and fastening systems were obtained in this effort [10], additional effort was required to generate a robust and repeatable method for collecting field bending strains. This additional effort is justified due to the fact that collecting and interpreting concrete sleeper flexural data from the field provides useful information for designing laboratory experiments, calibrating FE models, and developing more optimal designs for future concrete sleepers. As such, researchers in RailTEC at UIUC designed, developed, and deployed an instrumentation methodology to quantify the bending behavior of concrete sleepers under revenue service train traffic.

2. Background and methodology

2.1. Prior approaches to flexural demand quantification

An international review of prior instrumentation and experimental efforts aimed at quantifying in-field concrete sleeper bending moments revealed a limited number of deployments. Those projects identified used either embedded or surface strain gauges [10,14–16] as well as fiber optic sensors [17], deployed at either the proof-of-concept level or in a temporary fashion. A primary drawback to embedded strain gauge methods is the need to cast gauges into the sleeper during the manufacturing process, limiting the breadth of use. Additionally, the protection of the gauges is of great importance using either imbedded or surface methods given demanding loading and environmental conditions encountered in the rail industry, as was noted in earlier research conducted by UIUC [10]. Finally, Venuti [16] noted challenges related to signal noise and post processing of the data that were challenging to address using surface-deployed instrumentation, which must be overcome to ensure reliable information is obtained from the data collected.

2.2. Proposed instrumentation technology – surface strain gauges

Given manufacturing and breadth-of-use limitations to embedded strain gauging, and the fact that concrete surface strain gauging has proven reliable in other applications [18–21], it was chosen as the method of instrumentation for several large-scale field research projects at UIUC [22–26]. It is well documented that strain gauges are versatile instrumentation hardware that were implemented as early as the 1940s [27,28] and have long been used to monitor the performance of transportation facilities [29], with many applications associated with the domain of rail engineering [15,16,30–33].

Building on the aforementioned experiences, UIUC researchers selected 120-ohm strain gauges of type PFL-30-11-3LT from Texas Measurements [34]. This type of strain gauge (Fig. 1) is specifically designed for use with concrete materials, based on information obtained from the manufacturer [35].

Longer gauges are recommended for heterogeneous specimens such as concrete, as the gauge will bridge the varied elements of the specimen under investigation [37]. In this particular case, the large length of the gauge (30 mm) allows it to span multiple pieces of aggregate and sections of mortar paste within the concrete element, thus the strain being reported is an average strain, rather than a localized strain in a piece of aggregate or section of mortar paste [34]. For reference, typical maximum size for concrete sleeper aggregate is around 10 mm (0.4 in), 66.7% smaller than the strain gauge length.

There are, however, limitations to using surface strain gauges on concrete materials. One such limitation is the ability to accurately measure strain across cracks that open after the surface strain gauge is installed [20]. If the cracking strength of the object in question is likely to be exceeded during testing, another instrumentation type (e.g. crack opening gauges, digital image correlation [DIC], etc. should be considered. For the range of strains expected in concrete sleepers for this research effort, widespread cracking of specimens was not expected.

Data from strain gauges were collected using National Instruments (NI) compact data acquisition system (cDAQ), which provided compact and reliable hardware that would perform in a robust manner in the demanding field environment (Fig. 2) [24,38]. The instrumentation setup was designed to be temperature compensating to minimize error due to temperature fluctuations from direct sunlight, shading from passing trains, and seasonal climate conditions. Previous pilot efforts conducted by UIUC in both laboratory and field settings utilized this instrumentation technology, and it has proven to be both cost effective and reliable [10]. cDAQ output signals from instrumentation are recorded through a NI LabVIEW virtual instrument (VI) developed for the site-specific instrumentation associated with this experimental program (e.g. varied number of channels, data acquisition rate, number of modules, etc.).

Shielded wiring was used to minimize electrical interference and "cross talk" between the various channels of data being collected. Expert opinion and findings from prior research [16] has also indicated that this is especially critical in an environment that involves the use of electrified propulsion systems to avoid stray current concerns, as is the case with most light and heavy rail transit agencies.

A minimum sampling rate was determined based on the maximum authorized train speed at each field experimentation location and the desired data sampling resolution, where the sampling resolution is the distance the train travels along the track between consecutive samples. The sampling resolution desired for the example application discussed in this paper was 12.7 mm (0.5

Fig. 1. Standard 120-Ohm concrete strain gauge before left) and after right) installation on concrete sleeper [36].

Fig. 2. Compact Data Acquisition (cDAQ) chassis with interchangeable modules [38].

in.). Based on these requirements, prior experience, and expert recommendation, the sampling rate was set as 2000 Hz.

Prior experience and documentation from manufacturers [39] has shown the importance of providing adequate protection for the strain gauges, especially given the demanding field environment in which they are expected to perform reliably over long periods of time and accumulated gross tonnage of rail traffic. As such, the protection plan shown in Fig. 3 and explained in greater detail in Table 1 was implemented for each strain gauge placed on the concrete sleepers. Of special importance is the type of epoxy used to ensure that its expansion and contraction characteristics did not interfere with the data collection process, and Devcon 2-Ton® clear epoxy was found to be the best option given that it had similar thermal expansion properties as the substrate.

2.3. Instrumentation deployment on sleeper

Bending strains at critical discrete locations along the length of the sleeper were measured to quantify the flexural behavior of the sleeper under train loading. As such, concrete surface strain gauges were applied oriented longitudinally along the chamfer near the top surface of the sleeper. For a portion of the sleepers at each field testing location, a total of five strain gauges (labeled A – E) were used on each sleeper, with one applied at each of the two rail seats, one at the center, and another located approximately halfway between each rail seat and the sleeper center (Fig. 4). For the remainder of sleepers at most of the field experimentation sites, the two intermediate strain gauges were not installed, given the comparatively greater importance of capturing the center and rail seat moments. The dimensions shown in Fig. 4 account for a specific instrumented sleeper with a total length of 258 cm (102 in.), a common sleeper type used in the United States on heavy-haul freight railroads. Instrumented sleepers in the field with fully protected gauges can be seen in Fig. 5.

The most critical locations in terms of analyzing the flexural service demands on the sleeper are the sleeper center (Gauge C) and rail seat (Gauges A and E). To relate the measured strains to a bending moment, calibration factors were determined using two methods that are discussed in the next section.

3. Theory

3.1. Interpretation of data and generation of results

Measured sleeper strains from field sites and revenue service loading conditions must be correlated to bending moments using factors that are generated using one of three methods; (1) using a calibration constant from calculations based on known sleeper sectional geometries and concrete properties, (2) generating laboratory calibration curves by applying known moments under controlled experiments i.e. loading conditions and support configurations), or (3) calibrating each sleeper while they are installed in track [15]. The latter method was deemed impractical for UIUC's purposes given the number of required field sites and individual sleepers that would be instrumented and the safety and operational constraints of working in an active railway environment. The former two methods will be explored in greater detail in the following sections.

3.1.1. Laboratory calibration

Laboratory calibration was conducted using the Static Tie Tester (STT) (Fig. 5) at UIUC's Research and Innovation Laboratory (RAIL) in the Harry Schnabel Jr. Building in Champaign, IL, USA. The STT can apply known loads to test the flexural and/or compressive behavior of concrete sleepers. The STT uses a hydraulic cylinder to apply loads to the rail seat or center of a sleeper up to approximately 4450 kN (100,000 lbf). A calibrated load cell is used to monitor the applied loads to relate strain and bending moments.

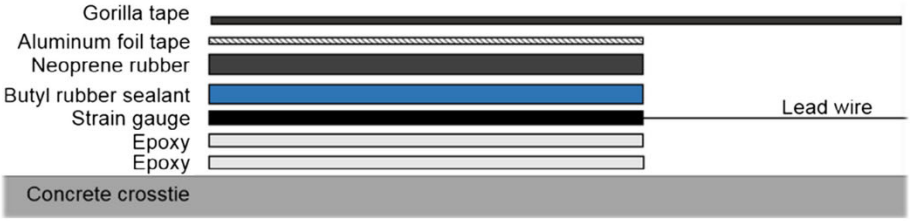

Fig. 3. Concrete surface strain gauge protection plan modified from [36].

Table 1
Explanation of strain gauge protection plan layers modified from [36].

Layer	Description	Purpose
Epoxy (Bottom)	Two-part epoxy, applied in two coats: primer and secondary	Primer coat bonds with concrete surface and provides smooth surface to mount strain gauge, secondary coat bonds strain gauge to primer
Strain gauge	Sensor that measures change in resistance caused by induced strains	Measures the change in strain experienced by the concrete under an applied load
Butyl rubber sealant	Sticky rubber layer	Provides moisture and mechanical protection for gauge
Neoprene rubber	Harder, stiffer rubber layer	Provides mechanical protection for gauge
Aluminum foil tape	Reflective tape layer	Provides moisture protection to gauge and holds all lower protection layers in place
Lead wire	Three-wire insulated bundled wire	Transmits strain signal recorded by gauge to data acquisition
Gorilla Tape® (Top)	Resilient tape layer	Holds all lower protection layers in place

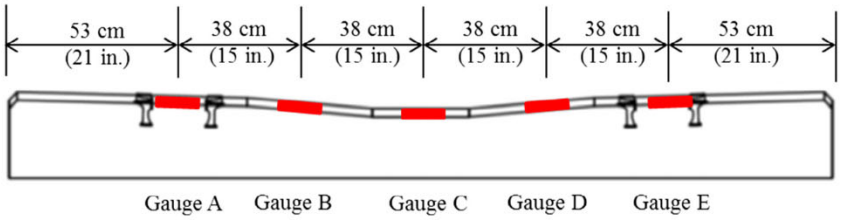

Fig. 4. Profile view of instrumented sleeper showing installation and locations of strain gauges modified from [36].

Fig. 5. Images of sleepers instrumented with concrete surface strain gauges at a heavy-haul freight railroad field experimentation location.

Fig. 6. Static Tie Tester (STT) at UIUC used for laboratory calibration of concrete sleepers.

Calibration of surface strain gauges requires a sleeper of the same design, strength, and approximate age to be instrumented with surface strain gauges through the procedure described above and then subjected to a known applied bending moment. Laboratory calibration included rail seat positive and negative bending tests and sleeper center positive and negative bending tests. Moments were applied by loading the sleeper using pre-established procedures outlined in Sections 4.9.1.4 and 4.9.1.6 of the American Railway Engineering and Maintenance-of-Way Association AREMA) Manual for Railway Engineering [40]. These procedures specify placement of supports and equations to be used to determine the moment induced in the sleeper from the load applied. Load and strain data were collected throughout the test so that researchers could determine relationship between strain and moment, calculated from applied load, for each sleeper. Tests were performed on the rail seat and center sections of each the sleeper, as shown in Figs. 7 and 8, respectively.

The calibration process uses the relationship described in Eq. (1) to relate a known bending moment to the concrete sleeper's sectional properties and response to load:

$$M_s = \frac{\varepsilon_s E_c I_s}{d_s} \tag{1}$$

where

M_s is the sleeper bending moment at section "s" (kN m (kip-in))
ε_s is the strain measurement taken from the surface strain gauge at section "s" (m/m (in/in))
E_c is the elastic modulus of the concrete (kPa (psi))
I_s is the moment of inertia at section "s" (m^4 (in^4))
d_s is the distance from the surface strain gauge to the neutral axis of bending of the sleeper at section "s" (m (in.))

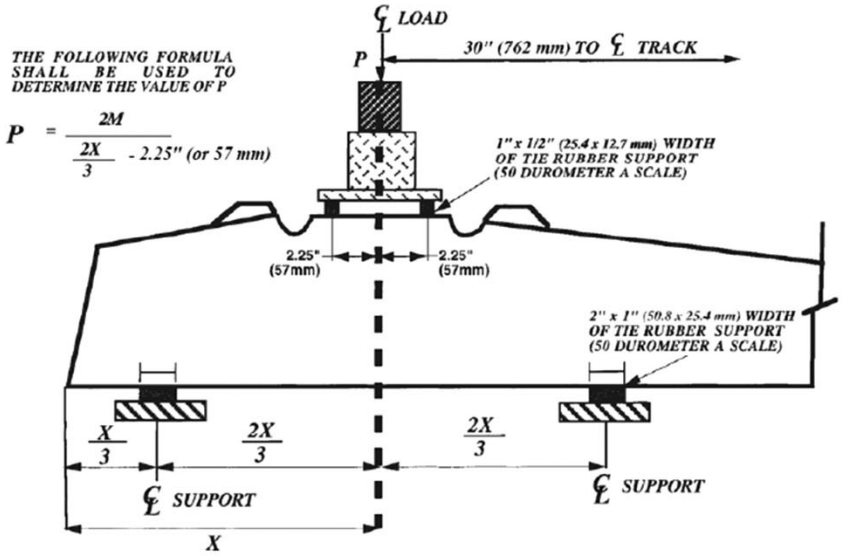

Fig. 7. Rail seat positive bending moment test protocol used for laboratory calibration of concrete sleepers AREMA [41].

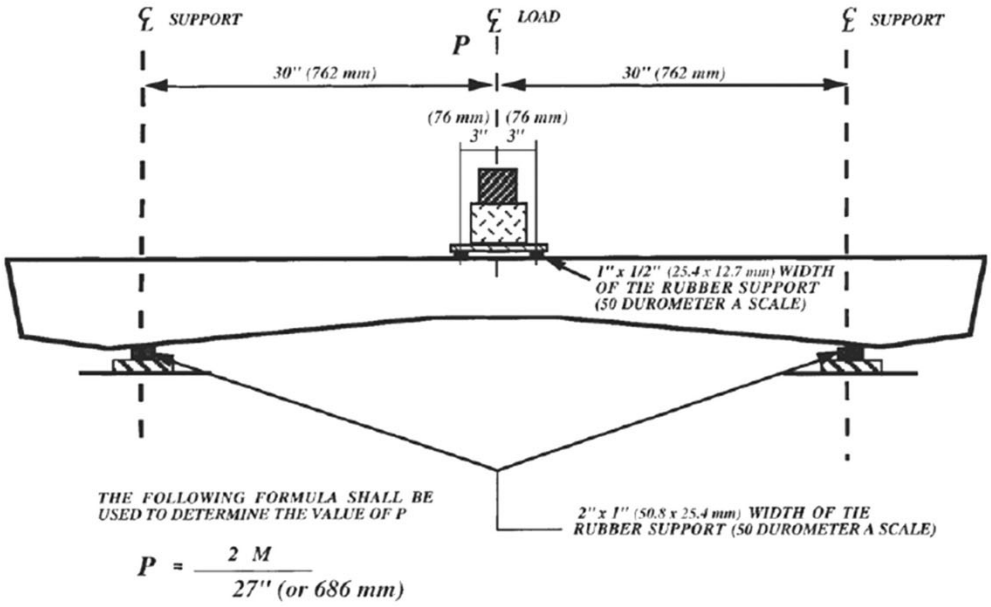

Fig. 8. Center negative bending moment test protocol used for laboratory calibration of concrete sleepers AREMA [41].

Section "s" refers to the cross-section of the sleeper where the strain gauge is located, which must be consistent between the calibration sleeper and the test sleeper in the field. The terms E_c, I_s, and d_s are unique to the sleeper and are determined in an aggregate fashion through laboratory calibration. For the experimentation that will be discussed in this paper to illustrate the measurement technique, the laboratory calibration factors were found to be 89,362.8 kN m/ε (790,927.6 kip-in/ε), 77,341.8 kN m/ε (684,532.8 kip-in/ε), and 66,878.1 kN m/ε (591,921.4 kip-in/ε) for Gauges A and E, Gauges B and D, and Gauge C, respectively.

Rail seat gauges were calibrated during the rail seat positive bending (Fig. 7) moment test and center and intermediate gauges were calibrated during the center negative bending moment test (Fig. 8). In order to minimize error and reduce variability, it was determined that three replicates of each calibration test should be conducted on each sleeper, and three sleepers of each design and age were tested, for a total of 9 test executions. Calibration loads were calculated such that the first crack design capacity of the sleeper would not be exceeded, as described by AREMA [40]. Specifications used for calibration of both types of concrete sleepers discussed in this paper can be found in Table 2.

An example of the laboratory calibration curves can be found in Fig. 9. Red data points shown in the figure represent the laboratory data recorded during an example sleeper center gauge calibration, and the blue dashed line corresponds to the linear best fit of the laboratory data. The slope of the dashed line is the laboratory calibration factor for the concrete crosstie center gauge, calculated to be 55,658.6 kN m/ε (492,620.3 kip-in/ε).

Finally, it should be noted that laboratory experimentation provided the opportunity to determine the adequacy and accuracy of strain gauge placement, addressing the question of whether a strain gauge located on the chamfer of the rail seat (compression side) of the sleeper could reliably capture rail seat positive bending.

Table 2
Geometric and prestress orientation properties required for calibration of concrete sleepers used in two example rail transit and Class I railroad freight applications.

Location	Property	Rail mode/system	
		Rail transit	Class I freight
Sleeper dimensions			
Overall	Length	2.6 m (8.5 ft)	2.6 m (8.5 ft)
	x-Value	53.3 cm (21.0 in)	53.3 cm (21.0 in)
Center	Depth	17.1 cm (6.8 in)	17.1 cm (6.8 in)
	Top Width	21.4 cm (8.4 in)	22.9 cm (9.0 in)
	Bottom Width	26.7 cm (10.5 in)	27.9 cm (11.0 in)
	Eccentricity	−1.0 cm (−0.4 in)	0.8 cm (0.3 in)
Rail seat	Depth	21.8 cm (8.56 in)	22.2 cm (8.8 in)
	Top Width	21.4 cm (8.44 in)	22.9 cm (9.0 in)
	Bottom Width	26.7 cm (10.5 in)	27.9 cm (11.0 in)
	Eccentricity	1.2 cm (0.459 in)	1.5 cm (0.6 in)

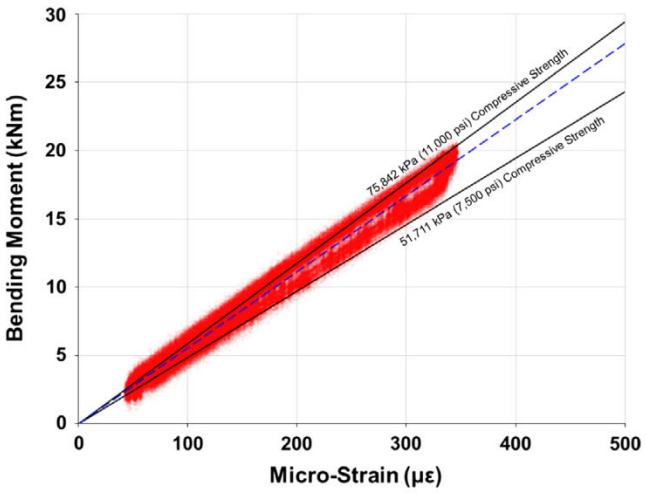

Fig. 9. Comparison of data from concrete sleeper center laboratory calibration (red scattered points) with analytical calculations (black lines) for a typical heavy haul freight sleeper. (For interpretation of the references to colour in this figure legend, the reader is referred to the web version of this article.)

3.1.2. Analytical calculations using fundamental equations

As shown in Eq. (1), the calibration factor is defined as $\frac{E_c I_s}{d_s}$, in which all of the terms can be calculated taking into account the geometric properties of the sleeper, the effect of prestressing the concrete, and the concrete material properties. Given that the sleeper's cross-section was simplified as an isosceles trapezoid as illustrated in Fig. 10, I_s was computed using Eq. (2). The effects of prestress, including the prestress force magnitude and the location and layout of the prestressing strands, were taken into consideration by eccentricity, which was defined as the distance between the center of gravity of the prestress wires and the neutral axis of the section. The neutral axis in Fig. 10 is shown to be higher than the center of gravity, indicating a negative eccentricity. However, depending on the prestress location and layout, the neutral axis can be lower than the center of gravity, creating a positive eccentricity.

$$I_s = \frac{h_s^3(a_s^2 + 4a_s b_s + b_s^2)}{36(a_s + b_s)} + e_s^2\left[\frac{h_s(a_s + b_s)}{2} + \left(\frac{E_{ps}}{E_c} - 1\right)A_{ps}\right] \quad (2)$$

where

a_s is the top width at section "s" (m (in.))
b_s is the bottom width at section "s" (m (in.))
h_s is the total depth at section "s" (m (in.))

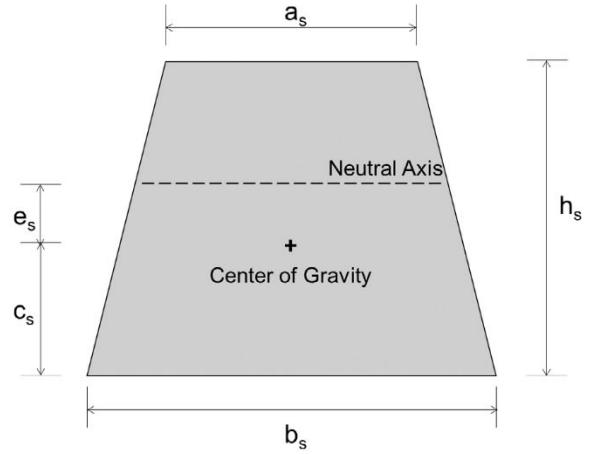

Fig. 10. Schematic showing example concrete sleeper cross-sectional view and location of critical sectional elements.

e_s is the eccentricity at section "s" (m (in.))
E_{ps} is the elastic modulus of the prestressing strands (kPa (psi))
E_c is the elastic modulus of the concrete (kPa (psi))
A_{ps} is the area of prestressing strands at section "s" (m^2 (in^2))

In order to calculate d_s, the location of the center of gravity was first determined based on the geometric properties of the sleepers (Eq. (3)). Next, d_s was determined using Eq. (4) in which the eccentricity was included in the computation.

$$c_s = \frac{h_s}{3}\left(\frac{2a_s + b_s}{a_s + b_s}\right) \quad (3)$$

wherec_s is the height of the center of gravity at section "s" (m (in.))

$$d_s = h_s + e_s - c_s - g_s \quad (4)$$

where

g_s is the vertical distance between the horizontal centerline of the surface strain gauge and the top of the sleeper at section "s" (m (in.))

Concrete compressive strength and concrete unit weight were both considered in the calculation of E_c (Eq. (5)). Conversations with United States sleeper suppliers led us to bound the expected range of concrete compressive strengths to a minimum of 51,711 kPa (7500 psi) and a maximum of 75,842 kPa (11,000 psi).

$$E_c = 0.043 w_c^{1.5}\sqrt{f'_c} \quad (5)$$

where

w_c is the unit weight of the concrete (kg/m^3)
f'_c is the concrete compressive strength (MPa)

After obtaining the sectional properties, the eccentricity, and the concrete normal weight, the calibration factor for the sleeper center was calculated to be 48,609.6 kN m/ε (430,231.5 kip-in/ε) at the minimum concrete compressive strength, and 58,847.1 kN m/ε (520,840.4 kip-in/ε) at the maximum compressive strength. The range of the calibration factors was depicted as the area between the two solid black lines in Fig. 9. The calibration factor obtained in the laboratory was located at the upper portion of the range, indicating that the concrete compressive strengths of the instrumented sleepers were closer to the maximum expected value. Given that the instrumented sleepers were previously in service for several years before they were taken out of the track for

this project, and concrete compressive strength tends to increase over time [42], the authors were comfortable with the consistent results obtained from both laboratory and hand calculation methods, although in some instances, found the laboratory calibrations to be more reliable. The interpretation of field bending moment results introduced in subsequent sections within article will use laboratory calibrations generated using the procedure referenced in this section.

4. Field instrumentation deployment

Between 2015 and 2017, seven field deployments using this technology have been installed by UIUC researchers throughout the United States to answer a variety of questions that require quantification of field concrete sleeper bending moments. To demonstrate the instrumentation methodology and repeatability of results, this article includes example data related to the quantification of bending moments for assessing sleeper-to-sleeper variability. Quantifying bending moment variability is a critical step in the development of future mechanistic recommendations [13] for concrete sleeper flexural design.

This specific field experimentation discussed in this manuscript was conducted on a ballasted heavy-haul freight railroad line in the western portion of the United States. Because of the high variability of support conditions seen in past field experimentation [10], instrumentation was placed in two locations, or "zones," of tangent (i.e. straight) track, spaced approximately 18.3 m (60 ft.) apart on center (Fig. 11). Each zone consisted of five concrete sleepers, based on the widely accepted theory on the distribution of vertical load to five consecutive sleepers [1,5] (Fig. 11). UIUC researchers predicted that the complete site of ten sleepers would adequately address the need for replicate data and provide insight into the variability of support conditions in this specific section of track.

5. Data analysis procedure

To quantify the bending moments concrete sleepers experience in revenue service, peaks in the strain gauge signal caused by sleeper bending due to a wheel or axle load must be extracted from the data stream collected at 2000 Hz. This was accomplished using the "findpeaks" function in MATLAB [43]. To improve the performance of this function for this application, several of the built-in options were utilized, and additional modifications were made to the code that was originally developed by Wolf [24]. To ensure that the true peaks were being captured by the program, as opposed to false peaks that did not represent the extreme strain reading for a given axle pass, a minimum spacing ("MinPeakDistance") between the peaks was specified and a minimum value ("MinPeakHeight") for all peaks was set. Before the peaks were obtained, the strain signal was zeroed using data captured before the arrival of the lead axle on the first locomotive, smoothed using a moving average filter of five data points, and a linear baseline correction was applied to adjust for any signal drift over the course of a single train pass. As such, data collection was initiated several seconds prior to the arrival of the leading axle of the first. This provided a stable zero point for the sleeper under no applied load. Additionally, the data collection was ended several seconds after the final train axle passed to serve as an end point for the baseline correction.

For instrumentation sites having a single train traffic type, the number of axles was a fixed value determined by the car configuration; for other sites, the number of axles was computed using a manually-adjusted "findpeaks" function. When the instrumentation sites were close to wheel impact load detectors (WILDs), a separate wayside inspection system used to measure vertical input loads at the wheel rail interface, the total number of axles could be obtained from the WILD data.

The value of "MinPeakDistance" was based on the axle spacing and train speed, whereas the value of "MinPeakHeight" was based on the axle load. Once the number of axles was determined, peaks could be pulled from all the strain gauge signals. The bisection method was implemented to shorten the processing time. For each strain gauge signal, the global maximum value was first obtained. This value was then halved and used as the "MinPeakHeight" in the "findpeaks" function. If the number of axles generated from the function was lower than the actual number, meaning that the "MinPeakHeight" was higher than some peaks, the "MinPeakHeight" would be further halved and used as the new input in the "findpeaks" function. If the number of axles generated from the function was greater than the actual number, indicating that the "MinPeakHeight" was lower than all peaks, the "MinPeakHeight" would be increased by half of its value and executed in the new "findpeaks" function. The iterations would stop once the output number of axles matched the actual axle count and all peaks were confirmed to have been extracted from the signal.

Fig. 12 (left vertical axis) shows an example of a typical strain gauge signal for a center gauge. The signal was zeroed out and the peaks were numbered in sequence, which were eventually converted into bending moments using the laboratory moment calibration factors mentioned previously (Fig. 12, right vertical axis).

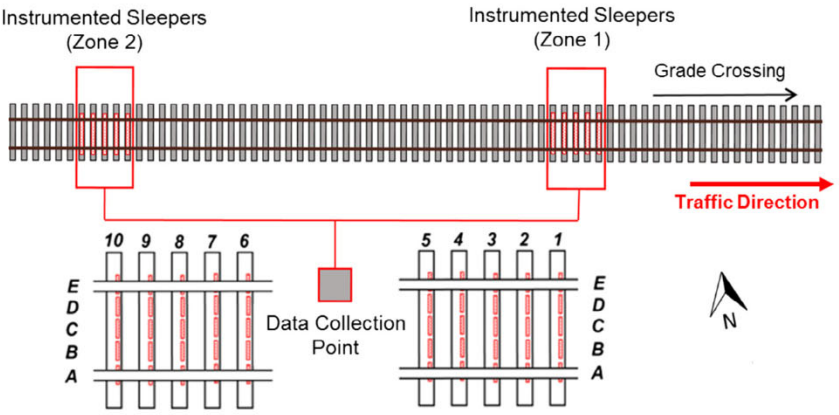

Fig. 11. Field experimentation site layout with ten sleepers in two test zones modified from [36].

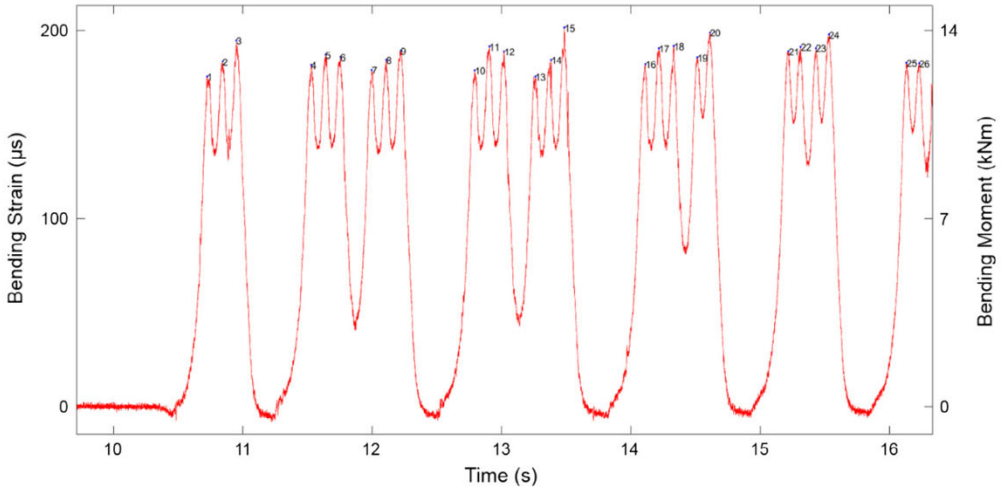

Fig. 12. Typical sleeper center strain signal and moment captured under the passage of a loaded heavy haul freight train (three six-axle locomotives and the first two 4-axle railcars).

6. Results

The instrumentation plan described in this article has proved to be robust, as only one surface strain gauge at this specific heavy-haul freight railroad site has been damaged over of the two-year time frame in which the field experimentation site has been operational and there have been no fatigue-related challenges with or failures of the strain gauges. Over the course of the site's functionality, approximately 267 million gross metric tons (295 million gross tons ((MGT)) of heavy-haul freight traffic have accumulated on the sleepers. Additionally, the other field sites have experienced similar successes in terms of instrumentation robustness, with minimal instrumentation-related failures.

For the purpose of the analysis described in this article, a total of 150 train passes containing over 80,000 individual axle passes were collected during the ten-day period from 30 December 2016 to 8 January 2017. UIUC researchers then analyzed the bending moments induced by loaded axles from the signals of the center and rail seat strain gauges (Gauges A, C, and E) mounted on all 10 sleepers. The bending moment percent exceeding distribution for the aforementioned 150 trains are shown in Fig. 13 to demonstrate the variability that is associated with consecutive train passes. These distributions are also shown in comparison to the AREMA recommended design limits for both rail seat positive and center negative cracking, effectively showing the moment that would need to be exceeded before a crack propagates to the first line of prestressing steel [40].

6.1. Overview of measured bending moments and selected findings

It is noticeable that the majority of the sleeper's average bending moments did not reach the AREMA recommended design limit shown with vertical black dashed lines (Fig. 13), especially at the rail seats, as their average moment values were less than one-third of the 33.9 kN m 300 kip-in) limit that AREMA recommends for sleeper flexural design [40]. This means that AREMA recommendations might overestimate the flexural demand at the sleeper rail seat section [40]. Compared to rail seat moments, average center bending moments were closer to the AREMA recommended value of 22.7 kN m 201 kip-in), with the moments for Sleeper 4 exceeding

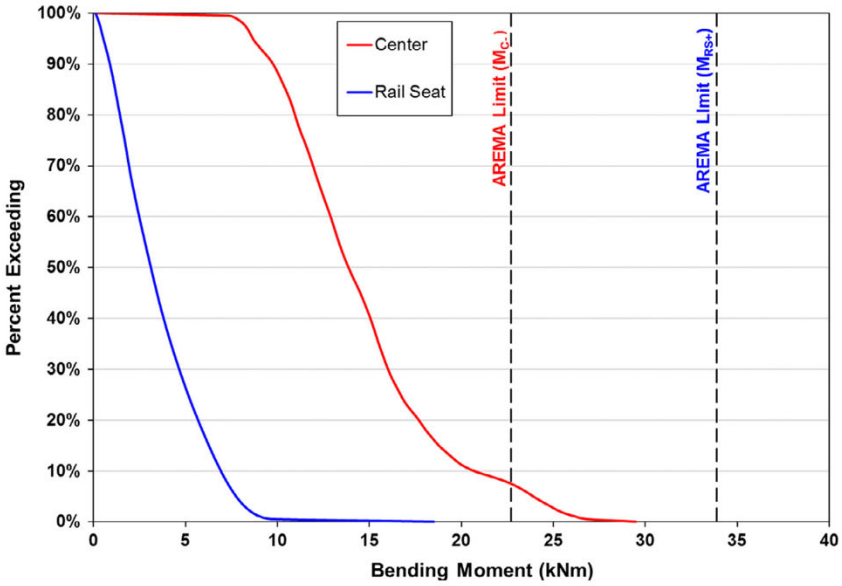

Fig. 13. Distribution of center and rail seat bending moments for each axle/wheel of all trains captured over a ten-day period in late 2016 and early 2017.

the AREMA recommended value, indicating that center bending could be more demanding than rail seat bending [40]. This agrees with the previous survey, which suggested that center cracking of concrete sleepers was more commonly seen in the field [5].

To best visualize the distribution of measured bending moments of each sleeper, box-and-whisker plots were developed (Fig. 14) for each sleeper. The top line of the box represents the 75th percentile bending moment (Q3). The middle line is the median bending moment. The bottom line of the box represents the 25 percentile bending moment (Q1). The interquartile range (IQR), found as Q3 minus Q1, can provide an estimate of the variability of the data set – the greater the IQR, the higher the variability. The upper whisker shown in Fig. 6 is the limit for upper outliers, which are defined as data points greater than Q3 plus 1.5 times the IQR (or $(Q3 + 1.5 * IQR)$) *(12)*. Similarly, the lower whisker is the limit for lower outliers, which are defined as data points smaller than Q1 minus 1.5 times the IQR or $Q1 - 1.5 * IQR)$) [44].

Sleeper 4's bending moment values suggest that the sleeper could have experienced a crack to the first level of prestress wires, entering into a range of flexural demand that this instrumentation technology may not be reliable in capturing. This cracking was visually confirmed by researchers during a site visit. The behavior of Sleeper 4 led to the conclusion that, while the overall behavior of sleepers was such that the flexural demands were below the design

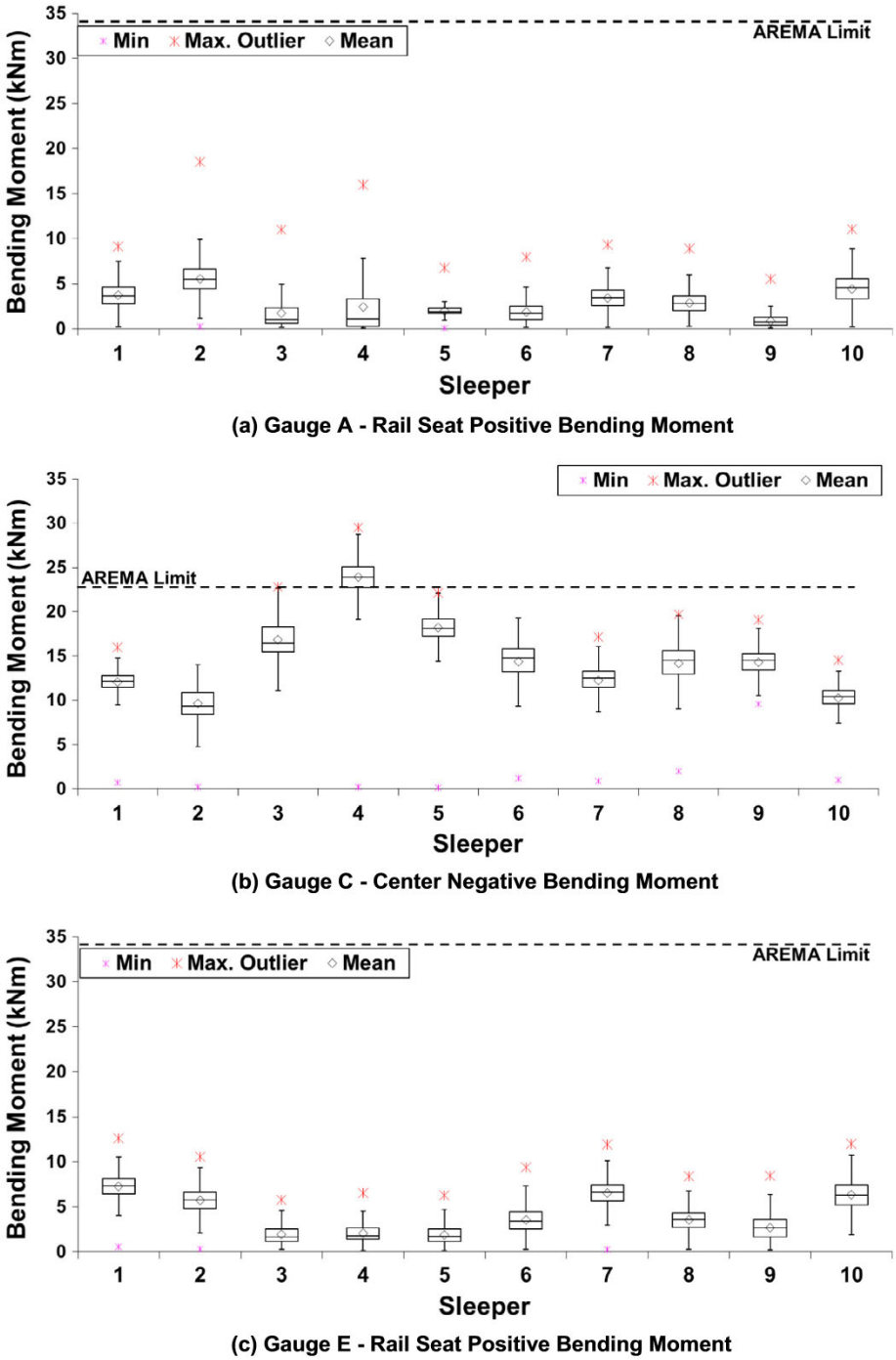

Fig. 14. Field data showing the variability of bending moments at three critical concrete sleeper locations on a heavy-haul freight railroad system.

limits, it is evident that the flexural demands can exceed design capacity in certain circumstances. These circumstances likely arise after settlement at the rail seats has generated a "center bound" condition that places excessive demand on the sleeper's center section. This condition can be predicted using the methodology introduced in this paper, and can be mitigated through track maintenance (i.e. tamping of ballast under sleeper to regain uniform support).

It is also important to note that even though the sleeper is cracked, potentially even below the first level of prestress, laboratory experimentation has shown that significant residual capacity remains and Sleeper 4 is likely to function normally for the foreseeable future [41]. When excluding Sleeper 4 for the aforementioned reasons, the probability of exceedance of the AREMA recommended practice value for center moment design was calculated to less than 0.5%.

To address the support condition question that led to the deployment of this instrumentation, as can be seen in Fig. 14, bending moment magnitudes for both sleeper centers and rail seats are quite variable from sleeper-to-sleeper, providing validation and quantification of our assumption of the variability in sleeper support conditions. The standard deviation of average rail seat bending moments and center bending moments are 1.86 kN m and 2.82 kN m, respectively. This likely indicates that center bending is more sensitive (i.e. variable) to support conditions than rail seat bending.

Finally, the data in Fig. 14 show that the maximum values of center bending moments (Fig. 14b) are closer to the AREMA design recommendations than maximum rail seat bending moments (Fig. 14a and b) indicating that the factor of safety for rail seats i.e. design value divided by the field readings) is less than the factor of safety at the sleeper center. This is of specific interest to the railway infrastructure design community, given AREMA [40] might overestimate the flexural demand on rail seats and that the design protocol could be better balanced to have similar safety factors for both critical design areas; the rail seat and the sleeper center.

7. Concluding remarks

This concrete surface strain gauge instrumentation methodology and deployment was successful in measuring the bending strains and resulting moments experienced by a variety of rail traffic in North America, and this paper has demonstrated their usefulness in quantifying sleeper-to-sleeper variability in a heavy-haul freight railroad revenue deployment. To date, the effectiveness of surface-mounted concrete strain gauges in measuring sleeper bending behavior has been demonstrated in the following railroad engineering applications, addressing the questions listed below:

- *Do the bending moments experienced by concrete sleepers vary from sleeper-to-sleeper?* This was demonstrated in this paper with respect to a heavy haul freight railroad application, showing bending moments at the sleeper center that ranged from 0 kN m (0 kip-in) to 22.8 kN m 202 kip-in) and similar results have been presented in prior papers [22,24,25].
- *Does accumulated train tonnage have an influence on the flexural demands of concrete sleepers?* Tonnage plays a role in the flexural demands on concrete sleepers, but while the measured moments were quantified correctly, the connection between the two is not as clear as hypothesized. The effects of tamping i.e. re-establishing the substructure/ballast under the sleeper) was clearly shown, supporting prevailing guidance on its usefulness at preventing center binding [22]. Specifically, sleeper center bending moments were observed to decrease by 63% after tamping.
- *Does temperature-induced* curl *(e.g. warping of the sleeper due to varied temperatures on the top and bottom) of concrete sleepers impact the flexural demand placed on the sleeper?* Curl in concrete sleepers was found to change over the course of the day as the temperature gradient changed. Temperature gradients were found to fluctuate and were mostly non-linear, and these changes affected the bending moments induced in the concrete sleepers [26,36], a behavior similar to that which has been noted in rigid pavement applications [45]. Due to the aforementioned temperature gradients, Wolf [24] noted changes in center negative bending moments of as much as 5 kN m (45 kip-in) representing nearly 25% of the sleeper's design capacity under changes in temperature gradient of less than 16.7 degrees Celsius (30 degrees Fahrenheit).

Acknowledgements

Portions of this research effort were funded by the Federal Railroad Administration (FRA), part of the United States Department of Transportation (US DOT). The material in this paper represents the position of the authors and not necessarily that of FRA. The authors would like to acknowledge the following industry partners: Union Pacific Railroad; BNSF Railway; National Railway Passenger Corporation (Amtrak); Progress Rail Services, a Caterpillar company; GIC; Hanson Professional Services, Inc.; and CXT Concrete Ties, Inc., an LB Foster Company. The authors would also like to formally thank Steve Mattson of voestalpine Nortrak, Prof. Bill Spencer and Sihang Wei of UIUC, Prof. Dan Kuchma of Tufts University, and Prof. Fernando Moreu of the University of New Mexico for their knowledge in instrumentation, and Matt Csenge, Phanuwat Kaewpanya, and Don Marrow for their assistance in the collection and processing of this data. J. Riley Edwards has been supported in part by grants to the UIUC's RailTEC from CN and Hanson Professional Services, Inc.

References

[1] W.W. Hay, Railroad engineering, 2nd ed., John Wiley & Sons, New York, NY, 1982.
[2] Railway Track and Structures, MW Budges to Rise in 2008. Railw. Track Struct., 2008.
[3] K. Senese, 2016 Annual Crosstie Update, Railw. Track Struct. (2016) 22–33.
[4] J.C. Zeman, Hydraulic mechanisms of concrete-tie rail seat deterioration, University of Illinois at Urbana-Champaign, 2010.
[5] B.J. Van Dyk, Characterization of the loading environment for shared-use railway superstructure in North America, University of Illinois at Urbana-Champaign, 2014.
[6] A.E. Naaman, Prestressed Concrete Analysis and Design: Fundamentals, second ed., Techno Press 3000, Ann Arbor, Mich., 2004.
[7] Jimenez, R., LoPresti, J., 2004. Performance of alternative tie material under heavy-axle-load traffic 16.
[8] L. Domingo, C. Zamorano Martín, C. Palenzuela Avilés, J.I. Real Herráiz, Analysis of the influence of cracked sleepers under static loading on ballasted railway tracks, Sci. World J. (2014) 1–10, http://dx.doi.org/10.1155/2014/363547.
[9] J.-A. Zakeri, F.H. Rezvani, Failures of railway concrete sleepers during service life, Int. J. Constr. Eng. Manag. 1 (2012) 1–5.
[10] J.R. Edwards, M.S. Dersch, R.G. Kernes, Improved Concrete Crosstie and Fastening Systems for US High Speed Passenger Rail and Joint Corridors (Federal Railroad Administration (FRA) No. Volume 1), 2017.
[11] J.S. Grassé, Field test program of the concrete crosstie and fastening system, University of Illinois at Urbana-Champaign, 2013.
[12] J.S. Grassé, S. Wei, J.R. Edwards, D. Kuchma, D.A. Lange, Field study of load path in rail and concrete crosstie system, Electron. J. Struct. Eng. (2014) 29–38.
[13] Van Dyk, B.J., Edwards, J.R., Ruppert Jr, C.J., Barkan, C.P., 2013. Considerations for mechanistic design of concrete sleepers and elastic fastening systems in North America, in: Proceedings of the 2013 International Heavy Haul Association Conference. p. 4.
[14] O. Kerokoski, T. Rantala, A. Nurmikolu, Deterioration mechanisms and life cycle of concrete monoblock railway sleepers in Finnish conditions, Italy, Milan, 2016.
[15] Ronald A. Mayville, Liying Jiang, Matthew Sherman, Performance Evaluation of Concrete Railroad Ties on the Northeast Corridor. Federal Railroad Administration, 2014.

[16] W. Venuti, Report on the Structural Response of the BART Concrete Ties, San Jose State University, San Jose, CA, 1990.
[17] Consolis, SMART SLEEPERS® A Concrete Sleeper with Accurate and Resistant Embedded Sensors, n.d.
[18] R. Chen, X. Zhao, Z. Wang, H. Jiang, X. Bian, Experimental study on dynamic load magnification factor for ballastless track-subgrade of high-speed railway, J. Rock Mech. Geotech. Eng. 5 (2013) 306–311, http://dx.doi.org/10.1016/j.jrmge.2013.04.004.
[19] Cheng, C., Bian, X., Jiang, H., Jiang, J., 2014. Model testing on dynamic behaviors of the slab track of high-speed railway, in: Proceedings of the 9th International Conference on Structural Dynamics, EURODYN 2014. Porto, pp. 813–818.
[20] J. Roesler, E. Barenberg, Fatigue and static testing of concrete slabs, Transp. Res. Rec. J. Transp. Res. Board 1684 (1999) 71–80, http://dx.doi.org/10.3141/1684-09.
[21] H. Yu, L. Khazanovich, M. Darter, A. Ardani, Analysis of concrete pavement responses to temperature and wheel loads measured from intrumented slabs. Transp. Res, Rec. J Transp. Res. Board (1998) 94–101.
[22] Z. Gao, H.E. Wolf, M.S. Dersch, Y. Qian, J.R. Edwards, Field measurements and proposed analysis of concrete crosstie bending moments, in: Proceedings of the American Railway Engineering and Maintenance of Way Association Annual Meeting, Orlando, Florida, 2016.
[23] H.E. Wolf, S. Mattson, J.R. Edwards, M.S. Dersch, C.P. Barkan, Flexural analysis of prestressed concrete monoblock crossties: comparison of current methodologies and sensitivity to support conditions, in: Proceedings of the Transportation Research Board 94th Annual Meeting, 2014.
[24] H.E. Wolf, Flexural Behavior of Prestressed Concrete Monoblock Crossties, University of Illinois at Urbana-Champaign, 2015.
[25] H.E. Wolf, J.R. Edwards, M.S. Dersch, C.P. Barkan, Flexural analysis of prestressed concrete monoblock sleepers for heavy-haul applications: methodologies and sensitivity to support conditions, in: Proceedings of the 11th International Heavy Haul Association Conference, 2015.
[26] H.E. Wolf, Y. Qian, J.R. Edwards, M.S. Dersch, D.A. Lange, Temperature-induced curl behavior of prestressed concrete and its effect on railroad crossties, Constr. Build. Mater. 115 (2016) 319–326, http://dx.doi.org/10.1016/j.conbuildmat.2016.04.039.
[27] R.L. Hannah, S.E. Reed, Strain Gage Users' Handbook, Springer Science & Business Media, 1992.
[28] A.L. Window, Strain Gauge Technology, Springer, Netherlands, 1992.
[29] A.S. Khan, X. Wang, Strain measurements and stress analysis, Prentice Hall, 2001.
[30] D. Cortis, M. Bruner, G. Malavasi, S. Rossi, M. Catena, M. Testa, Estimation of the wheel-rail lateral contact force through the analysis of the rail web bending strains, Measurement 99 (2017) 23–35, http://dx.doi.org/10.1016/j.measurement.2016.12.015.
[31] B. Stratman, Y. Liu, S. Mahadevan, Structural health monitoring of railroad wheels using wheel impact load detectors, J. Fail. Anal. Prev. 7 (2007) 218–225, http://dx.doi.org/10.1007/s11668-007-9043-3.
[32] W. Venuti, Field Investigatoin of the Gerwick RT-7 Prestress Concrete Tie, San Jose State University, 1970.
[33] S.K. Yang, T.S. Liu, Y.C. Cheng, Automatic measurement of payload for heavy vehicles using strain gages, Measurement 41 (2008) 491–502, http://dx.doi.org/10.1016/j.measurement.2007.07.003.
[34] Vishay Micro-Measurements, Strain gage selection: criteria, procedures, recommendations, 2007.
[35] TML, 2017. Developing Strain Gauges and Instruments.
[36] H.E. Wolf, Application of Surface Strain Guages, University of Illinois at Urbana-Champaign, 2015.
[37] HBN, 2017. Strain Gauges.
[38] National Instruments, CompactDAQ, 2017.
[39] Vishay Micro-Measurements, Strain gage installations for concrete structures, 2007.
[40] AREMA, AREMA Chapter 30 (Ties), in: Manual on Railway Engineering. Landover, MD, 2016.
[41] J.C. Bastos, Analysis of the performance and failure of railroad concrete crossties with various track support conditions, University of Illinois at Urbana-Champaign, 2016.
[42] S. Mindess, J.F. Young, D. Darwin, Concrete, Prentice Hall, 2003.
[43] MATLAB, MATLAB and Statistics Toolbox Release, The MathWorks Inc, Natick, Massachusetts, United States, 2012.
[44] R.L. Ott, M. Longnecker, An Introduction to Statistical Methods and Data Analysis,, 6 ed., Brooks/Cole, Australia; United States, 2008.
[45] C. Beckemeyer, L. Khazanovich, H. Thomas Yu, Determining amount of built-in curling in jointed plain concrete pavement: case study of Pennsylvania 1–80, Transp. Res Rec. J Transp. Res. Board (2002) 85–92.